Emittance sharing and exchange driven by linear betatron coupling in circular accelerators

A. Franchi, E. Métral, and R. Tomás

CERN, Geneva, Switzerland
(Received 4 April 2007; published 21 June 2007)

The influence of linear betatron coupling due to constant-in-time skew quadrupolar fields on the transverse emittances is discussed using both a simplified model of a smooth circular accelerator and a more realistic strong-focusing lattice with localized sources of coupling (thin lens). New formulas for the coupled transverse emittances are derived that include the initial emittances, the coupling strengths, and the tune distance from the resonance. By using the more powerful Lie algebra and the resonance driving terms formalism, equivalent formulas are derived that provide a better understanding of some counterintuitive effects, otherwise not understandable in the smooth approximation. The new formulas have been tested both numerically and experimentally by using data of the CERN Proton Synchrotron showing a remarkable agreement.

PACS numbers: 29.20.−c

I. INTRODUCTION

Emittance transfer between the transverse planes in circular accelerators has been widely studied in the framework of betatron linear coupling [1–3]. The understanding of this mechanism is of help to optimize the multiturn injection, as well as to prevent beam losses driven by aperture limitations. Similar studies, mainly focused on transport lines, have been carried out in the matrix notation by employing the second-order beam moments matrix [4–6].

Equations governing the emittance transfer have been already derived from single-particle differential equations, in the smooth approximation and assuming a uniformly distributed skew quadrupolar field [1,2]. A more general treatment has been also derived in the **C** matrix formalism [3], leading to relations straightforward to implement numerically, but difficult to exploit in terms of observables.

Emittance transfer has been studied mainly in the *static case*, where the tunes $Q_{x,y}$ are constant. The two emittances execute fast oscillations whose (time) averaged value depends on the distance from the resonance,

$$\Delta = Q_x - Q_y - l, \qquad l \in \mathbf{N}, \tag{1}$$

where l is the integer difference between the betatron tunes. Equal averaged emittances at maximum can be obtained on the resonance, $\Delta = 0$.

In [7] it was observed experimentally that the dynamic crossing of the above resonance leads to a complete emittance exchange between the two planes, $\epsilon_{xf} = \epsilon_{y0}$ and $\epsilon_{yf} = \epsilon_{x0}$, where ϵ_0 and ϵ_f are the root mean square (RMS) emittances at the beginning and at the end of the crossing, respectively.

In this paper we provide the theoretical description of this effect, in the smooth approximation as well as in a strong-focusing lattice. Formulas able to predict the emittance exchange are eventually derived. The only assumptions made here are that the dynamic crossing is slow

enough to make the particle distribution be always matched and that the term driving the sum resonance $Q_x + Q_y - l = 0$ is negligible. The first condition is essential for the derivation of the new formulas when computing the RMS emittance ϵ_x from the single-particle emittance E_x. The second condition is necessary to guarantee that the sum of the two emittances is invariant. The assumption of having weak coupling is no longer necessary here as no truncation is introduced. The effects due to the synchrotron motion, chromaticity, and dispersion are not considered. Nevertheless, the comparison between analytic formulas and experimental data from the CERN Proton Synchrotron (PS) (bunched beam with normalized chromaticity $\xi = Q'/Q \simeq -1$ and nonzero dispersion) shows a remarkable agreement. In machines with unsplit tunes ($l = 0$), when the space-charge forces are no longer negligible, even in the absence of linear betatron coupling similar effects of emittance sharing and exchange have been observed, both in numerical simulations [8] and in measurements [9]. The analysis of the space-charge forces and of any other nonlinear effects (such as amplitude dependent detuning) is left outside the scope of this paper.

In Sec. II the existing theory of the emittance sharing as described in [1,2] is reviewed.

In Sec. III we derive analytical expressions describing the emittance exchange, by solving the coupled differential equations in the smooth approximation and assuming a uniformly distributed skew quadrupole field.

In Sec. IV we apply the resonance driving term (RDT) formalism as illustrated in [10] to derive analogous equations describing the emittance transfer as a function of the RDT, in the static as well as in the dynamic case. These new relations describe the emittance transfer to higher accuracy than the existing formulas. The advantage of this approach is that the assumption of having a smooth lattice is removed. The counterintuitive emittance variation around the ring due to localized sources of coupling observed in multiparticle simulations is shown to be the

A. FRANCHI, E. MÉTRAL, AND R. TOMÁS

Phys. Rev. ST Accel. Beams **10,** 064003 (2007)

consequence of the analogous variation of the RDT. Explicit relations connecting the matrix and the RDT approaches were given in [11].

In Sec. V several possible methods to compute and measure the RDT responsible for the emittance exchange are outlined, by either using beam position monitors (BPMs) or emittance monitors.

In Sec. VI the comparison between the theoretical predictions and the emittance-exchange curves measured in the PS by means of wire scanners is carried out.

II. EXISTING THEORY OF EMITTANCE SHARING IN THE SMOOTH APPROXIMATION (STATIC CASE)

The static approach of the resonance refers to the exploration of the resonance stop band in several machine cycles. From cycle to cycle the tune in one plane is usually varied, keeping the other fixed. Both tunes remain constant during each cycle. Close to the resonance, the transverse planes share their RMS emittances. The shared amount depends on the coupling strength and the distance from the resonance. On the resonance the two emittances (averaged over several turns) are equal, i.e. $\epsilon_x = \epsilon_y$. Analytic formulas were previously derived [1,2] for a constant focusing lattice whose s-dependent coupling strength $j(s)$ is replaced by a uniform coupling strength given by [12]

$$C = -\frac{1}{2\pi} \oint ds\, j(s) \sqrt{\beta_x(s)\beta_y(s)}\, e^{-i[\phi_x(s)-\phi_y(s)]+i(s/R)\Delta},$$

(2)

where R is the machine radius, s is the longitudinal coordinate, β and ϕ are the Twiss parameters of the uncoupled lattice, and Δ the fractional distance from the resonance of the bare tunes defined in Eq. (1). Up to the first order $|C|$ is equivalent to the "tune difference on the coupling resonance", $\Delta Q_{\min}$ (also known as the "closest tune approach"). The transverse RMS emittances, averaged over a number of turns $N \gg 1/|C|$, are coupled according to

$$\epsilon_x = \epsilon_{x0} + \frac{|C|^2}{\Delta^2 + |C|^2} \frac{\epsilon_{y0} - \epsilon_{x0}}{2}$$

(3)

$$\epsilon_y = \epsilon_{y0} - \frac{|C|^2}{\Delta^2 + |C|^2} \frac{\epsilon_{y0} - \epsilon_{x0}}{2}.$$

(4)

These equations were derived in the 1970s [1,2] with the aim of increasing the injection efficiency of both the CERN PS and the PS Booster, by *redistribution* during injection of the (larger) horizontal emittance to the vertical plane. In Fig. 1 the RMS emittances from multiparticle simulations are plotted versus Δ and compared with Eqs. (3) and (4) for two different amounts of coupling, $|C| = 0.01$ and $|C| = 0.002$, respectively. In the later case the RMS curves show
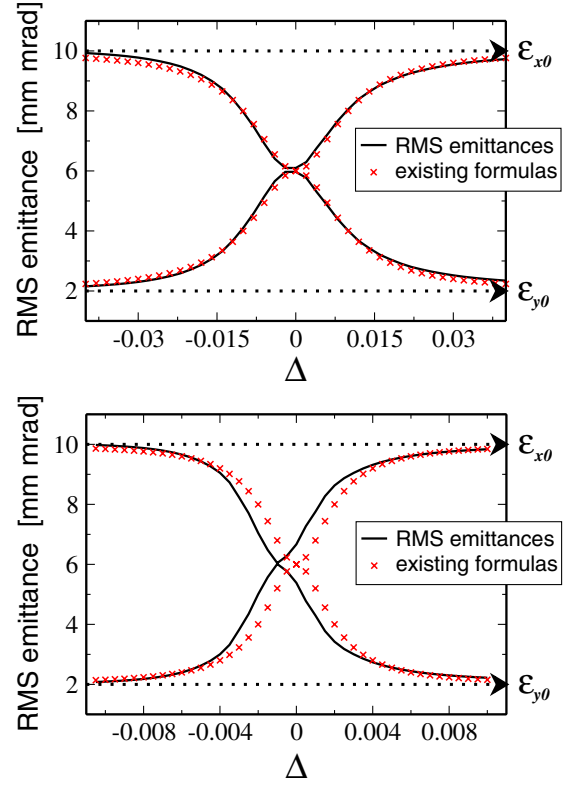

FIG. 1. (Color) RMS emittances against $\Delta = Q_x - Q_y - l, l \in \mathbf{N}$ from multiparticle simulations compared with Eqs. (3) and (4) for $|C| = 0.01$ (top) and $|C| = 0.002$ (bottom).

an asymmetry not foreseen by the existing formulas in Eqs. (3) and (4). This asymmetry will be explained by the formalism of Sec. IV C. Note that in [1,2] fast oscillations have been ignored (as it is done by those emittance monitors that integrate the signal over a few ms). Therefore no information about the amplitude of these fast oscillations can be derived from Eqs. (3) and (4).

All the multiparticle simulations whose results are shown in this paper have been performed by using the MICROMAP libraries [13]. The reference lattice is a FODO cell consisting of 12 superperiods with tunes separated by one integer. Betatron coupling is generated by random skew quadrupolar components at the end of each focusing quadrupole.

III. NEW THEORY OF EMITTANCE EXCHANGE IN THE SMOOTH APPROXIMATION (DYNAMIC CASE)

Consider first the case near the resonance $Q_x - Q_y = 0$ (unsplit tunes). In this case, the equation of betatron motion in the smooth approximation, after performing the Floquet transformation, reads [2,14]

$$\frac{d^2 h_x}{d\phi^2} + Q_x^2 h_x = R^2 \underline{J}_1 h_y,$$

(5)

$$\frac{d^2 h_y}{d\phi^2} + Q_y^2 h_y = R^2 \underline{J}_1 h_x, \tag{6}$$

where $h_x = \hat{x} - i\hat{p}_x$ and $h_y = \hat{y} - i\hat{p}_y$ are the same complex Courant-Snyder coordinates of [15]. ϕ substitutes s as independent variable and is defined as follows:

$$\phi(s) = Q_x^{-1} \int_0^s \beta_x^{-1}(t)dt \approx Q_y^{-1} \int_0^s \beta_y^{-1}(t)dt. \tag{7}$$

In the smooth approximation with unsplit tunes, $Q_x \approx Q_y = Q_0$, $\beta_x \approx \beta_y \approx R/Q_0$. The coupling strength $\underline{J}_1$ (denoted sometimes in the literature by $\underline{K}_0$) is defined by the skew quadrupolar magnetic field B_x, the charge state Ze, and beam momentum p, according to $\underline{J}_1 = (Ze/p) \times (\partial B_x/\partial x)$. The coupling coefficient defined in Eq. (2) is proportional to $\underline{J}_1$, as in this case it reduces to

$$|C| = \frac{R^2}{Q_0} |\underline{J}_1|. \tag{8}$$

In the absence of coupling, the solutions of the homogeneous Eqs. (5) and (6) are given by

$$h_x = \sqrt{E_{x0}} e^{iQ_x\phi}, \qquad h_y = \sqrt{E_{y0}} e^{iQ_y\phi}. \tag{9}$$

In the presence of coupling, Eqs. (5) and (6) can be solved by searching the normal (i.e. decoupled) modes (u, v), which are linked to (h_x, h_y) by a simple rotation

$$\begin{pmatrix} h_x \\ h_y \end{pmatrix} = \begin{pmatrix} \cos\alpha & -\sin\alpha \\ \sin\alpha & \cos\alpha \end{pmatrix} \begin{pmatrix} u \\ v \end{pmatrix}, \tag{10}$$

where α is the angle between the two coordinate system. Replacing (h_x, h_y) by (u, v) in Eqs. (5) and (6) yields the equations of the two normal modes,

$$\frac{d^2 u}{d\phi^2} + Q_u^2 u = 0, \tag{11}$$

$$\frac{d^2 v}{d\phi^2} + Q_v^2 v = 0, \tag{12}$$

where

$$Q_u = Q_x - \frac{|C|}{2} \tan\alpha, \tag{13}$$

$$Q_v = Q_y + \frac{|C|}{2} \tan\alpha, \tag{14}$$

assuming small tune shifts, and

$$\tan 2\alpha = \frac{C}{\Delta}. \tag{15}$$

The solutions of Eqs. (11) and (12) are given by

$$u = \sqrt{2I_x} e^{iQ_u\phi}, \qquad v = \sqrt{2I_y} e^{iQ_v\phi}, \tag{16}$$

where I_x and I_y are constants of motion, which depend on

the initial conditions. Initially, the two planes are considered decoupled (there is a coupling strength $|C|$ constant, but $\Delta \gg |C|$). The normal modes (u, v) are thus equal to (h_x, h_y), and therefore $\sqrt{2I_x} = \sqrt{E_{x0}}$ and $\sqrt{2I_y} = \sqrt{E_{y0}}$. Applying Eq. (10) the complex Courant-Snyder coordinates can be found:

$$h_x = \sqrt{E_{x0}} e^{iQ_u\phi} \cos\alpha - \sqrt{E_{y0}} e^{iQ_v\phi} \sin\alpha, \tag{17}$$

$$h_y = \sqrt{E_{x0}} e^{iQ_u\phi} \sin\alpha + \sqrt{E_{y0}} e^{iQ_v\phi} \cos\alpha. \tag{18}$$

By definition, the horizontal and vertical "single-particle" emittances are given by

$$E_x = |h_x|^2, \qquad E_y = |h_y|^2. \tag{19}$$

One thus deduces from Eqs. (17) and (18) that

$$E_x = E_{x0}\cos^2\alpha + E_{y0}\sin^2\alpha - \Theta, \tag{20}$$

$$E_y = E_{x0}\sin^2\alpha + E_{y0}\cos^2\alpha + \Theta, \tag{21}$$

$$\Theta = \sqrt{E_{x0}E_{y0}} \sin 2\alpha \cos[(Q_u - Q_v)\phi],$$

where E_{x0} and E_{y0} are the initial uncoupled single-particle transverse emittances. It can be seen from Eqs. (20) and (21) that in the presence of linear coupling (close to the difference resonance) the sum of the single-particle emittances is always conserved:

$$E_x + E_y = E_{x0} + E_{y0}. \tag{22}$$

To obtain the RMS emittances of the beam, a first average over time (which is equivalent to an average over ϕ) and a second one over the particles in the beam have to be performed. The first average gives

$$\overline{E}_x = E_{x0}\cos^2\alpha + E_{y0}\sin^2\alpha, \tag{23}$$

$$\overline{E}_y = E_{x0}\sin^2\alpha + E_{y0}\cos^2\alpha. \tag{24}$$

Note that on the coupling resonance $Q_u - Q_v = |C|$. The oscillation period of the cosine term in Eqs. (20) and (21) is thus $T_\phi = 2\pi/|C|$. If $|C|$ is infinitely small, then an infinitely long time is needed to cross the resonance to average this term to 0. The second average yields

$$\epsilon_x = \epsilon_{x0}\cos^2\alpha + \epsilon_{y0}\sin^2\alpha, \tag{25}$$

$$\epsilon_y = \epsilon_{x0}\sin^2\alpha + \epsilon_{y0}\cos^2\alpha. \tag{26}$$

The sum of the rms emittances is thus also conserved:

$$\epsilon_x + \epsilon_y = \epsilon_{x0} + \epsilon_{y0}. \tag{27}$$

Using the fact that

$$\cos 2\alpha = \cos\left[\arctan\left(\frac{|C|}{\Delta}\right)\right] = \left(1 + \frac{|C|^2}{\Delta^2}\right)^{-1/2}, \tag{28}$$

it can be shown that

$$\sin^2\alpha = \frac{1}{2}\frac{|C|^2}{\Delta^2 + |C|^2 + |\Delta|\sqrt{\Delta^2 + |C|^2}}, \quad (29)$$

and Eqs. (25) and (26) can be rewritten:

$$\epsilon_x = \epsilon_{x0} + \frac{|C|^2}{\Delta^2 + |C|^2 \pm \Delta\sqrt{\Delta^2 + |C|^2}}\frac{\epsilon_{y0} - \epsilon_{x0}}{2}, \quad (30)$$

$$\epsilon_y = \epsilon_{y0} - \frac{|C|^2}{\Delta^2 + |C|^2 \pm \Delta\sqrt{\Delta^2 + |C|^2}}\frac{\epsilon_{y0} - \epsilon_{x0}}{2}. \quad (31)$$

It can be shown that the sign in the denominator depends on the crossing direction. Equations (30) and (31) are very similar to those obtained in the static case by Guignard [2]: there is only an additional term $\Delta(\Delta^2 + |C|^2)^{1/2}$ in the denominator. This term is however very important, as it makes possible the exchange of the transverse emittances after the resonance crossing.

From Eqs. (30) and (31) it is seen that far from the resonance stop band, i.e., when $\Delta \gg |C|$, the transverse emittances are given by

$$\epsilon_x = \epsilon_{x0}, \, \epsilon_y = \epsilon_{y0}. \quad (32)$$

As the tunes approach the resonance condition, $\Delta \approx 0$, the sharing of the emittances increases and reaches its maximum value for full coupling, where the emittances are given by

$$\epsilon_x = \epsilon_y = \frac{\epsilon_{y0} + \epsilon_{x0}}{2}. \quad (33)$$

After the resonance crossing, far from the stop band, $-\Delta \gg |C|$, the transverse emittances have been exchanged:

$$\epsilon_x = \epsilon_{y0}, \qquad \epsilon_y = \epsilon_{x0}. \quad (34)$$

As can be seen from Eqs. (30) and (31), the emittance is exchanged through the following function:

$$g(|C|, \Delta) = \frac{|C|^2}{\Delta^2 + |C|^2 \pm \Delta\sqrt{\Delta^2 + |C|^2}}, \quad (35)$$

which varies from 0 (before the crossing) to 1 (after the crossing), and is equal to 1/2 on the resonance, $\Delta = 0$. There the exchange speed is given by

$$\left|\frac{\partial g}{\partial \Delta}\right|(|C|, \Delta = 0) = \frac{1}{2|C|}. \quad (36)$$

This implies that, for a given resonance crossing $\Delta(t)$, the smaller the coupling strength, the faster the emittance exchange.

Note that Eqs. (5) and (6), as well as the derivation presented in this section, apply for the case with unsplit tunes only. Multiparticle simulations and recent measure-ments [7,16] show however that Eqs. (30) and (31) hold as well for machines with a different integer part of the betatron tunes. In [14], an expansion into Fourier series has been proposed to retrieve the same results for a generic coupling resonance $Q_x - Q_y - l = 0$, l being any integer. In the following sections we make use of the RDT formalism to avoid any assumptions regarding both the tune separation and the lattice structure.

IV. RESONANCE DRIVING TERM DESCRIPTION OF THE EMITTANCE SHARING AND EXCHANGE

In this section we extend the above results to the more general case of a strong-focusing lattice with localized sources of coupling (skew quadrupolar field). Normal forms and RDT have been proven in [10,15,16] to be a powerful tool to investigate lattice nonlinearities. This formalism is used here to describe betatron coupling close to the difference resonance. A closed Lie expansion for the particle coordinates is found which leads to a very general expression for both the single-particle and the RMS emittances.

A. Betatron motion close to the difference resonance

In the Appendix, the turn-by-turn evolution of the complex Courant-Snyder coordinates $h_{x,y}$ in a lattice with betatron coupling is computed by applying the Lie algebra. It is proven that, when the term driving the sum resonance is negligible with respect to the one driving the difference resonance, $|f_{1010}| \ll |f_{1001}|$, the betatron motion is described by the following relations:

$$h_x(N) = \cos(2f)\sqrt{2I_x}e^{i(2\pi NQ_u + \psi_{x0})}$$
$$- ie^{iq}\sin(2f)\sqrt{2I_y}e^{i(2\pi NQ_v + \psi_{y0})}, \quad (37)$$

$$h_y(N) = \cos(2f)\sqrt{2I_y}e^{i(2\pi NQ_v + \psi_{y0})}$$
$$- ie^{-iq}\sin(2f)\sqrt{2I_x}e^{i(2\pi NQ_u + \psi_{x0})}, \quad (38)$$

where N is the turn number, $I_{x,y}$ and $\psi_{x0,y0}$ are the normal form single-particle invariants and initial phases, respectively, whereas $Q_{u,v}$ are the eigentunes. f and q are the amplitude and the phase of the RDT f_{1001}, respectively, defined by

$$f_{1001} = fe^{iq}. \quad (39)$$

In first approximation f_{1001} depends on the integrated gradients of all the skew quadrupoles in the ring $J_{w,1}$, $w = 1, 2, 3, \dots, W$, on the Twiss parameters, and on the observation point labeled by b, according to [17]

$$f_{1001}^{(b)} = \bar{f}_{1001}^{(b)} + O(J_{w,1}^2), \quad (40)$$

$$\bar{f}^{(b)}_{1001} = \frac{\sum_w^W J_{w,1}\sqrt{\beta_x^w \beta_y^w}e^{i(\Delta\phi^b_{w,x} - \Delta\phi^b_{w,y})}}{4(1 - e^{2\pi i(Q_u - Q_v)})}, \qquad (41)$$

where $\Delta\phi^b_w$ is the phase advance of the skew quadrupole number w with respect to the position b. The difference between the above definition and the one given in [17] is that here the eigentunes $Q_{u,v}$ appear instead of the bare tunes $Q_{x,y}$. The substitution makes the quasiresonant $\bar{f}_{1001}$ not to diverge for $\Delta \to 0$. In Sec. V it will be shown how $\bar{f}_{1001} \approx f_{1001}$ as long as the tune working point is outside the stop band. To the first order in $J_{w,1}$, eigentunes and bare tunes coincide, as the detuning is a second-order effect, $Q_{u,v} = Q_{x,y} + O(J^2_{w,1})$.

It is important to stress the point that in the RDT formalism the resonance condition is defined through the complex term $e^{2\pi i(Q_u - Q_v)}$, which is independent of the tune separation l. Therefore all the results derived in this and the following sections apply to all lattices regardless of the tune separation. Another consequence is that only the fractional parts of the tunes should be carried on, when this complex term is expanded in Taylor series.

In matrix notation the system (38) and (39) reads

$$\begin{pmatrix} h_x(N) \\ h_y(N) \end{pmatrix} = \mathbf{F}\begin{pmatrix} \sqrt{2I_x}e^{i(\psi_{x0} + 2\pi N Q_u)} \\ \sqrt{2I_y}e^{i(\psi_{y0} + 2\pi N Q_v)} \end{pmatrix}, \qquad (42)$$

$$\mathbf{F} = \begin{pmatrix} \cos(2f) & -ie^{iq}\sin(2f) \\ -ie^{-iq}\sin(2f) & \cos(2f) \end{pmatrix}.$$

The system evaluated at $N = 0$ and inverted yields

$$\begin{pmatrix} \sqrt{2I_x}e^{i\psi_{x0}} \\ \sqrt{2I_y}e^{i\psi_{y0}} \end{pmatrix} = \mathbf{F}^{-1}\begin{pmatrix} \sqrt{E_{x0}}e^{i\phi_{x0}} \\ \sqrt{E_{y0}}e^{i\phi_{y0}} \end{pmatrix}, \qquad (43)$$

where we made explicit $h(0) = \sqrt{E_0}e^{i\phi_0}$, with E_0 and ϕ_0 the initial single-particle emittance and phase in the Cartesian coordinates, respectively. Note that Eq. (43) is the generalization of Eq. (10): in fact it can be shown that if the tunes are unsplit, $q \approx \pi/2$ and the two matrices are the same after replacing $2f = \alpha$. Equation (43) shows also the dependence of the invariants on the initial emittances and on f_{1001},

$$\sqrt{2I_x} = |\sqrt{E_{x0}}e^{i(\phi_{x0} - \phi_{y0} - q)}\cos(2f) + i\sqrt{E_{y0}}\sin(2f)|, \qquad (44)$$

$$\sqrt{2I_y} = |\sqrt{E_{y0}}e^{i(\phi_{y0} - \phi_{x0} + q)}\cos(2f) + i\sqrt{E_{x0}}\sin(2f)|. \qquad (45)$$

In the presence of betatron coupling $2I_{x,y}$ replace the single-particle emittances $E_{x,y}$ as invariant.

B. Static case: Single-particle emittances

The single-particle emittances $E_{x,y}(N) = |h_{x,y}(N)|^2$ can be described in terms of the normal form invariants.

Equations (38) and (39) indeed yield

$$E_x(N) = \cos^2(2f)(2I_x) + \sin^2(2f)(2I_y) + \Phi, \qquad (46)$$

$$E_y(N) = \cos^2(2f)(2I_y) + \sin^2(2f)(2I_x) - \Phi, \qquad (47)$$

$$\Phi = \sqrt{2I_x 2I_y}\sin(4f)\sin[q - (\psi_{x0} - \psi_{y0}) - 2\pi N(Q_u - Q_v)]. \qquad (48)$$

The sum of the two emittances reads

$$E_x(N) + E_y(N) = 2I_x + 2I_y = E_{x0} + E_{y0}, \qquad (49)$$

and it is constant in time. In order to remove the dependence of $E_{x,y}$ on $I_{x,y}$ and to make explicit the dependence on the initial emittances, we substitute Eq. (43) in Eq. (42). The complex Courant-Snyder variables are therefore given by

$$h_x(N) = \sqrt{E_{x0}}e^{i(2\pi N Q_u + \phi_{x0})}[\cos^2(2f) + e^{-i2\pi N\Delta_e}\sin^2(2f)]$$
$$+ i\frac{\sqrt{E_{y0}}}{2}e^{i(2\pi N Q_v + \phi_{y0} + q)}\sin(4f)[e^{i2\pi N\Delta_e} - 1], \qquad (50)$$

$$h_y(N) = \sqrt{E_{y0}}e^{i(2\pi N Q_v + \phi_{y0})}[\cos^2(2f) + e^{i2\pi N\Delta_e}\sin^2(2f)]$$
$$+ i\frac{\sqrt{E_{x0}}}{2}e^{i(2\pi N Q_u + \phi_{x0} - q)}\sin(4f)[1 - e^{-i2\pi N\Delta_e}], \qquad (51)$$

where $\Delta_e = Q_u - Q_v$ is the distance from the resonance of the eigentunes (fractional part). The single-particle emittances become

$$E_x(N) = E_{x0} + \sin^2(4f)[1 - \cos(2\pi N\Delta_e)]\frac{E_{y0} - E_{x0}}{2} + \mathbf{R}(\phi_{x0}, \phi_{y0}), \qquad (52)$$

$$E_y(N) = E_{y0} - \sin^2(4f)[1 - \cos(2\pi N\Delta_e)]\frac{E_{y0} - E_{x0}}{2} - \mathbf{R}(\phi_{x0}, \phi_{y0}), \qquad (53)$$

where $\mathbf{R}(\phi_{x0}, \phi_{y0})$ is a linear combination of $\sin(\phi_{x0} - \phi_{y0})$ and $\cos(\phi_{x0} - \phi_{y0})$.

C. Static case: RMS emittances

Turn-by-turn RMS emittances are computed by averaging the single-particle emittances given in Eqs. (52) and (53) over the particle distribution. The transverse matching condition results in a particle distribution $\rho(I_x, I_y)$ which is independent of the phases $\phi_{x,y}$. Therefore the average of $\mathbf{R}(\phi_x, \phi_y)$ cancels out, yielding

A. FRANCHI, E. MÉTRAL, AND R. TOMÁS

Phys. Rev. ST Accel. Beams **10,** 064003 (2007)

$$\epsilon_x(N) = \epsilon_{x0} + \sin^2(4f)\{1 - \cos(2\pi N\Delta_e)\}\frac{\epsilon_{y0} - \epsilon_{x0}}{2},$$

(54)

$$\epsilon_y(N) = \epsilon_{y0} - \sin^2(4f)\{1 - \cos(2\pi N\Delta_e)\}\frac{\epsilon_{y0} - \epsilon_{x0}}{2},$$

(55)

where as usual $f = |f_{1001}|$. Note that the above relations are independent of q. The two emittances oscillate in time (i.e. in N) with frequency $2\pi\Delta_e$. On the resonance the frequency is $\omega_0 = 2\pi|\Delta Q_{min}|$, with $|\Delta Q_{min}| \approx |C|$ the tune separation at $\Delta = 0$. These oscillations cannot be detected by any hardware integrating the signal over many turns. As done in Sec. III, a further averaging over $N \gg 1/|C|$ can be performed to derive an *averaged* RMS emittance. The time integration removes the oscillating term if Δ_e does not depend on time (static case), yielding

$$\epsilon_x = \epsilon_{x0} + \sin^2(4|f_{1001}|)\frac{\epsilon_{y0} - \epsilon_{x0}}{2}$$

(56)

$$\epsilon_y = \epsilon_{y0} - \sin^2(4|f_{1001}|)\frac{\epsilon_{y0} - \epsilon_{x0}}{2}.$$

(57)

In Fig. 2 the turn-by-turn RMS emittances from multi-particle simulations are plotted for $|C| = 0.128$ and three different working points. The closer Δ is to 0, the larger the amount of shared emittance is and the slower the exchange frequency is. The pictures show that the upper (in x) and lower (in y) crests are determined by the initial emittances only, as the exchange is due to a beam rotation in the $x - y$ plane. The emittance *redistribution* therefore applies only at the level of averaged emittances (horizontal lines).

Equations (3) and (4) are obtained from Eqs. (56) and (57) under several approximations. First it is convenient to introduce a new quantity, C_0, defined as follows:
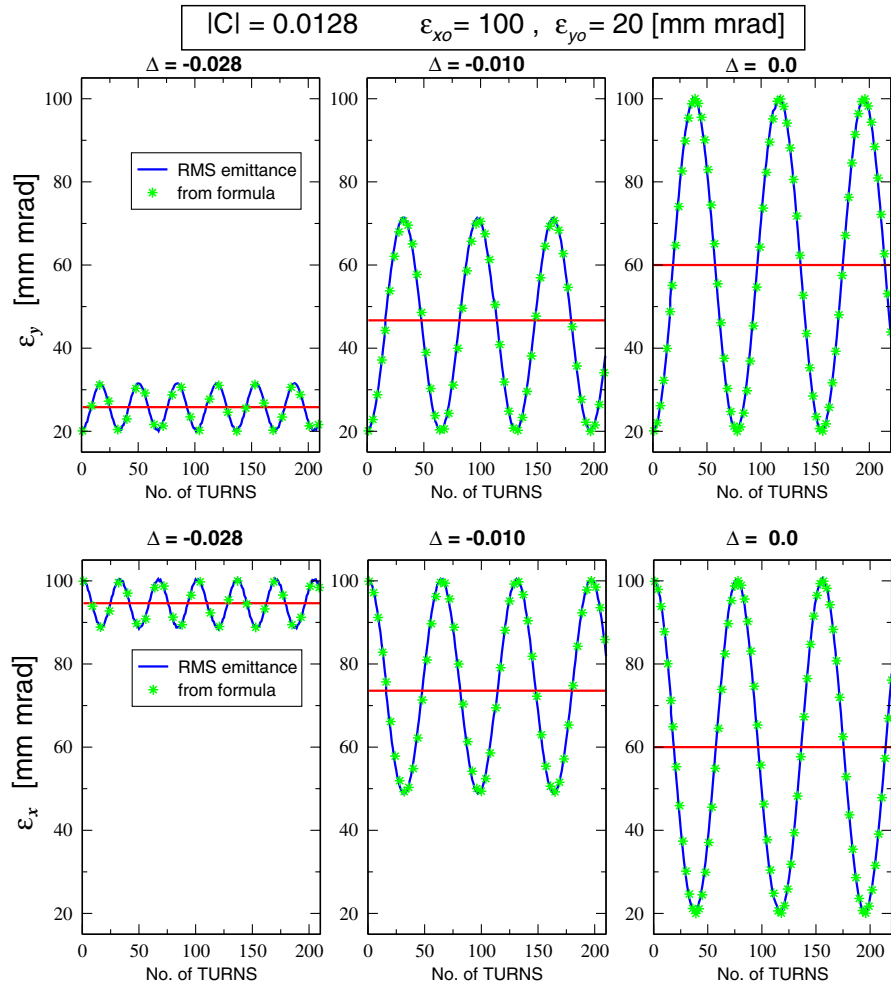

FIG. 2. (Color) Vertical (top) and horizontal (bottom) turn-by-turn RMS emittance ($|C| = 0.0128$). Simulations are repeated for three working points $\Delta = 0.028, 0.01, 0.0$. Horizontal lines correspond to the *average* RMS emittance. Stars are derived from Eqs. (54) and (55).
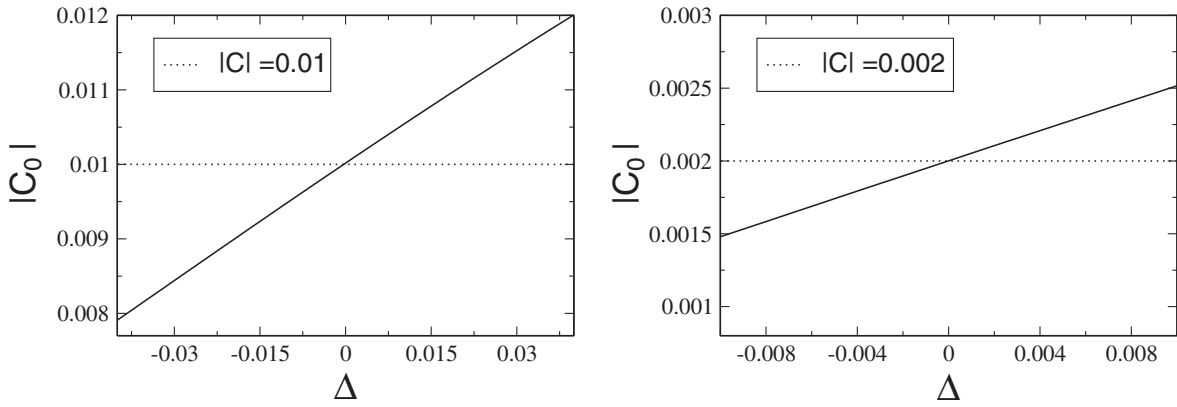
FIG. 3. $|C_0|$ against Δ for $|C| = 0.01$ (left) and $|C| = 0.002$ (right).

$$C_0 = -\frac{1}{2\pi} \oint ds\, j(s)\sqrt{\beta_x(s)\beta_y(s)}\, e^{-i(\phi_x(s)-\phi_y(s))}. \quad (58)$$

In the thin-lens approximation $j(s) = \sum_w J_{w,1}\delta(s - s_w)$, where δ is the Dirac function, yielding

$$|C_0| = \frac{1}{2\pi}\left|\sum_w J_{w,1}\sqrt{\beta_x^w \beta_y^w}\, e^{i(\phi_{w,x}-\phi_{w,y})}\right|. \quad (59)$$

The phase $e^{is/R\Delta}$ inside the integral in Eq. (2) (absent in C_0) makes $|C|$ independent of Δ. In the case of a single skew quadrupole driving betatron coupling, as well as in the smooth approximation, $|C_0| = |C|$. Instead in case of several localized skew quadrupoles $|C_0|$ exhibits a dependence on Δ. For $\Delta \ll 1$ this dependence appears to be linear as shown in Fig. 3. Assuming the observation point b at the origin, from Eq. (40) we obtain

$$|\bar{f}_{1001}| = \frac{2\pi|C_0|}{8|\sin(\pi\Delta_e)|} \approx \frac{|C_0|}{4|\Delta_e|}, \quad (60)$$

where we expanded $\sin(\pi\Delta_e) \approx \pi\Delta_e$, as $\Delta_e \ll 1$. Expanding the sine up to the first order in Eqs. (56) and (57) and replacing $f_{1001} \approx \bar{f}_{1001}$, we obtain

$$\sin^2(4|f_{1001}|) \approx 16|\bar{f}_{1001}|^2 \approx \frac{C_0^2}{\Delta_e^2}. \quad (61)$$

After substituting $\Delta_e^2 \approx \Delta^2 + |C|^2$, Eqs. (56) and (57) eventually read

$$\epsilon_x = \epsilon_{x0} + \frac{1}{2}\frac{|C_0|^2}{\Delta^2 + |C|^2}(\epsilon_{y0} - \epsilon_{x0}), \quad (62)$$

$$\epsilon_y = \epsilon_{y0} - \frac{1}{2}\frac{|C_0|^2}{\Delta^2 + |C|^2}(\epsilon_{y0} - \epsilon_{x0}). \quad (63)$$

Equations (3) and (4) are obtained expanding $|C_0|^2$ as Taylor series around $\Delta = 0$, namely $|C_0|^2 \approx |C|^2 + O(\Delta)$. Note that the approximation made in Eq. (61) provides a way to compute the maximum error $|f_{1001}| - |\bar{f}_{1001}|$: for $\Delta \to 0$, $|C_0| \to \Delta_e$ and $|\bar{f}_{1001}| \to 1/4$, whereas imposing that $\sin^2(4|f_{1001}|) = 1$, one concludes that $|f_{1001}| \to \frac{\pi}{8}$.

In Fig. 4 our new formulas (56) and (57) are compared with the simulated RMS emittances and the predictions from the previous model, Eqs. (3) and (4): for a coupling $|C| = 0.01$ both formulas follow the RMS values, whereas for $|C| = 0.002$ only the new formulas describe properly the sharing curve.

D. Static case: Emittance variation around the ring

Equations (54) and (55) reveal a counterintuitive aspect of the emittance behavior around the ring: in [10,11,16] it
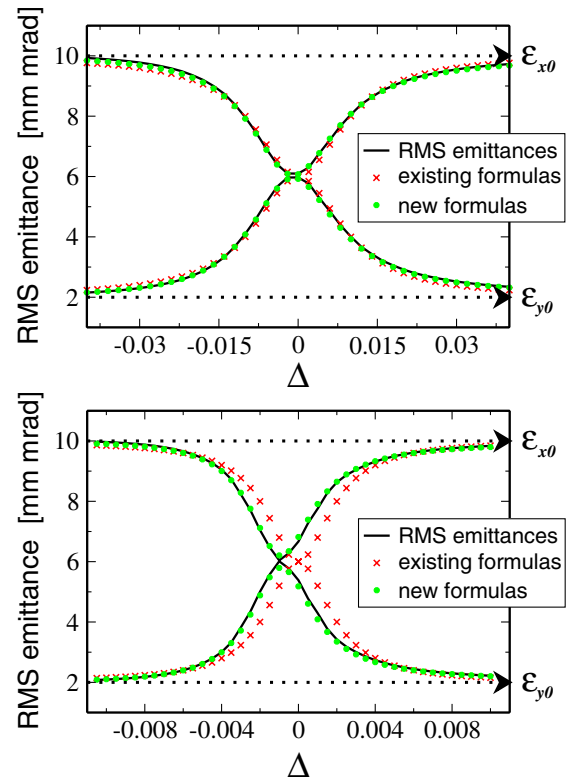

FIG. 4. (Color) The same RMS emittances of Fig. 1 compared with Eqs. (3) and (4) and the new formulas, Eqs. (56) and (57), for $|C| = 0.01$ (top) and $|C| = 0.002$ (bottom).

A. FRANCHI, E. MÉTRAL, AND R. TOMÁS

Phys. Rev. ST Accel. Beams **10,** 064003 (2007)

was shown how $|f_{1001}|$ remains constant in regions free of betatron coupling, whereas it exhibits abrupt jumps after a localized source of coupling. This is due to the presence of the betatron phase advances $\Delta\phi_w^b$ in Eq. (40), which renders the sum in the numerator dependent on the observation point b. Approaching the resonance conditions, these jumps become less visible, and $|f_{1001}|$ tends to remain constant around the ring. Jumps of $|f_{1001}|$ result in variations of the amount of shared emittance around the ring, according to Eqs. (54) and (55). This is indeed confirmed by multiparticle simulations shown in Fig. 5: the vertical RMS emittance is plotted turn by turn at three different locations of the ring, for different Δ and for two different amounts of coupling. ϵ_y (at any location) oscillates with frequency $\omega_N = 2\pi\Delta_e$. The lower crest is also independent of the position: this occurs when $\cos(2\pi N\Delta_e) = 1$ in Eqs. (54) and (55), regardless on the local value of $|f_{1001}|$. On the other hand, the upper crest occurs when $\cos(2\pi N\Delta_e) = 0$ and its value depends on the local value of $|f_{1001}|$; the relative difference tends to zero

approaching the resonance, as $|f_{1001}|$ remains constant around the ring.

E. Dynamic case: Single-particle emittances

In [16] it is shown how the matrix of Eq. (42) defines a transformation that decouples the system into the two normal modes. The amplitudes of the later ones, $2I_{x,y}$, replace hence the single-particle emittance $E_{x,y}$ as an adiabatic invariant when a slow tune variation is performed. Numerical simulations show that on the resonance $\Delta = 0$ the two invariants exchange abruptly (see left plot of Fig. 6). This exchange is related to the change in q (the phase of f_{1001}) by π as shown in the right plot of Fig. 6. Details of the numerical computation of both $2I_{x,y}$ and f_{1001} from single-particle simulations can be found in Sec. V. Since Eq. (40) holds outside the resonance stop band only, it cannot be used for a rigorous proof of this phase jump, which hence must be considered here as a heuristic starting point for the next derivation. To show
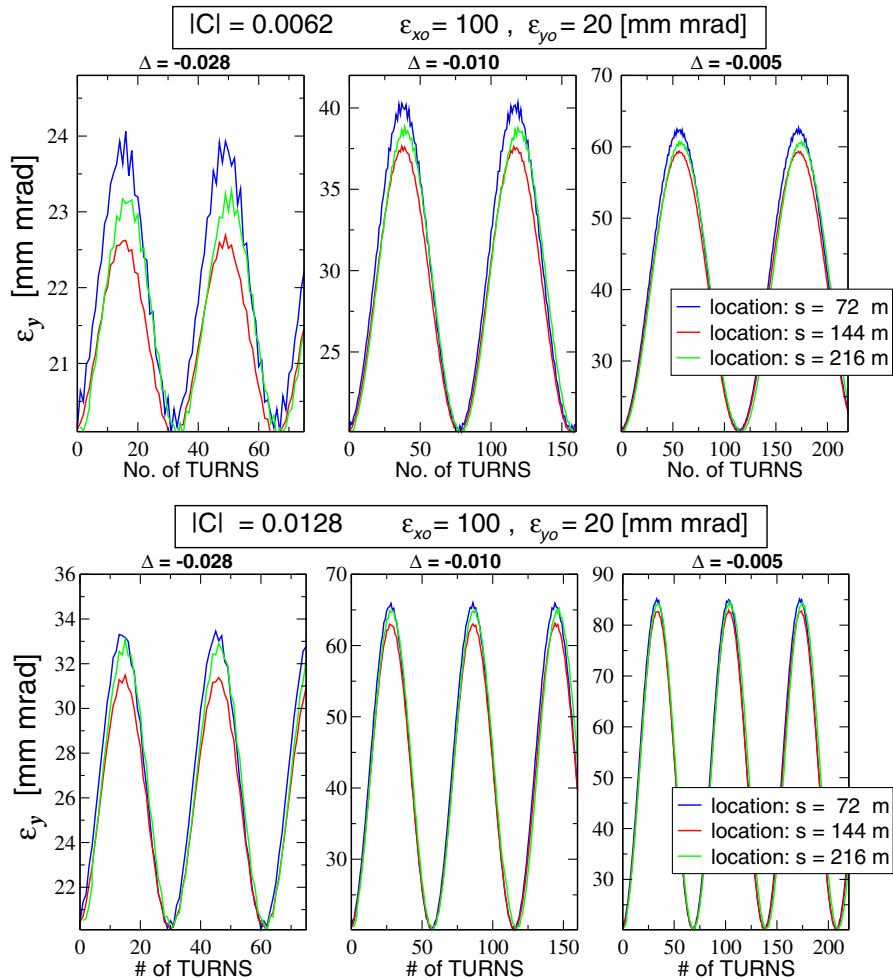

FIG. 5. (Color) Multiparticle simulations of the turn-by-turn RMS emittance oscillations for two different amounts of coupling and three working points. The three lines correspond to different locations where the emittances were computed.
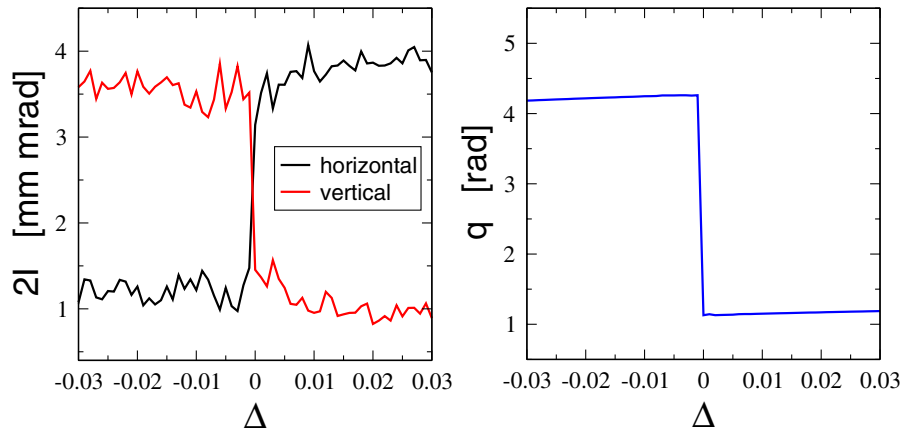
FIG. 6. (Color) Single-particle invariants, $2I_{x,y}$ (left) and phase of f_{1001} q (right) against $\Delta = Q_x - Q_y - l$, during the resonance crossing (numerical simulation).

how this abrupt exchange occurs, we compute $2I_{x,y}$ from Eqs. (44) and (45):

$$2I_x = \cos^2(2f)E_x + \sin^2(2f)E_y + \Theta, \qquad (64)$$

$$2I_y = \cos^2(2f)E_y + \sin^2(2f)E_x - \Theta, \qquad (65)$$

$$\Theta = \sqrt{E_x E_y} \sin(4f) \sin(\phi_x - \phi_y - q),$$

where as usual $f_{1001} = fe^{iq}$. Note that all the quantities in the right-hand side (rhs) of the equations above refer no longer to their initial values, as done in Eqs. (44) and (45). This is justified by the fact that the Twiss parameters $\phi_{x,y}$, the emittances $E_{x,y}$ and the RDT f_{1001} vary by slowly changing the tunes, whereas $2I_{x,y}$ remain constant. The sum and the difference of the invariants read, respectively,

$$2I_x + 2I_y = E_x + E_y = E_{x0} + E_{y0}, \qquad (66)$$

$$2I_x - 2I_y = \cos(4f)(E_x - E_y) + 2\Theta. \qquad (67)$$

Close to the resonance, i.e. $\Delta \approx 0$ and $f \approx \pi/8$, the tune working points $\Delta = \pm\delta$, where $\delta \approx 0$, are not equivalent since

$$(2I_x - 2I_y)|_{-\delta} = +2\sqrt{E_x E_y} \sin(\phi_x - \phi_y - q),$$
$$\qquad (68)$$

$$(2I_x - 2I_y)|_{\delta} = -2\sqrt{E_x E_y} \sin(\phi_x - \phi_y - q). \qquad (69)$$

Indeed according to our ansatz $q(\delta) = q(-\delta) - \pi$, whereas $\phi_{x,y}(\delta) \approx \phi_{x,y}(-\delta)$. The crossing therefore makes the difference change sign, while the sum remains constant. This is equivalent to saying that the crossing makes $2I_x$ and $2I_y$ exchange. The two invariants C_1 and C_2 and Eqs. (46) and (47) therefore read

$$C_1 = 2I_x \qquad C_2 = 2I_y \qquad \text{before crossing,} \qquad (70)$$

$$C_1 = 2I_y \qquad C_2 = 2I_x \qquad \text{after crossing,} \qquad (71)$$

$$E_x = \cos^2(2f)C_1 + \sin^2(2f)C_2 + \Phi, \qquad (72)$$

$$E_y = \cos^2(2f)C_2 + \sin^2(2f)C_1 - \Phi, \qquad (73)$$

$$\Phi = \sqrt{C_1 C_2} \sin(4f) \sin[q - (\psi_{x0} - \psi_{y0}) - 2\pi N \Delta_e].$$

F. Dynamic case: RMS emittances

The computation of the RMS emittances requires the knowledge of the RMS values of $C_{1,2}$. The adiabatic condition can be invoked to keep the particle distribution always matched and therefore independent of the betatron phases. As for the static case, when the RMS values are computed, terms proportional to $\sin(\phi_{x0} - \phi_{y0})$ and $\cos(\phi_{x0} - \phi_{y0})$ cancel out. Equations (64) and (65) evaluated at $N = 0$ yield

$$\begin{cases} c_1 = \cos^2(2f_0)\epsilon_{x0} + \sin^2(2f_0)\epsilon_{y0}, \\ c_2 = \cos^2(2f_0)\epsilon_{y0} + \sin^2(2f_0)\epsilon_{x0}, \end{cases} \qquad (74)$$

where f_0, ϵ_{x0}, and ϵ_{y0} are the initial absolute value of f_{1001} and RMS emittances, respectively. The average over $N \gg 1/|C|$ cancels out Φ and the *averaged* RMS emittances eventually read

$$\epsilon_x = c_1 + \sin^2(2|f_{1001}|)(c_2 - c_1), \qquad (75)$$

$$\epsilon_y = c_2 - \sin^2(2|f_{1001}|)(c_2 - c_1), \qquad (76)$$

where c_1 and c_2 exchange after crossing the resonance. It can be shown that the above relations are equivalent to

$$\epsilon_x = c_h + T_f(c_v - c_h), \qquad (77)$$

$$\epsilon_y = c_v - T_f(c_v - c_h), \qquad (78)$$

where

$$c_h = \cos^2(2f_0)\epsilon_{x0} + \sin^2(2f_0)\epsilon_{y0}, \qquad (79)$$

$$c_v = \cos^2(2f_0)\epsilon_{y0} + \sin^2(2f_0)\epsilon_{x0}, \qquad (80)$$

$$T_f = \begin{cases} \sin^2(2|f_{1001}|) & \text{before crossing} \\ \cos^2(2|f_{1001}|) & \text{after crossing.} \end{cases} \qquad (81)$$

With this notation the exchange of the invariants is implicit in T_f whereas c_h and c_v remain constant.

Note that the above relations hold for a starting point not necessarily far from the resonance, a mandatory condition
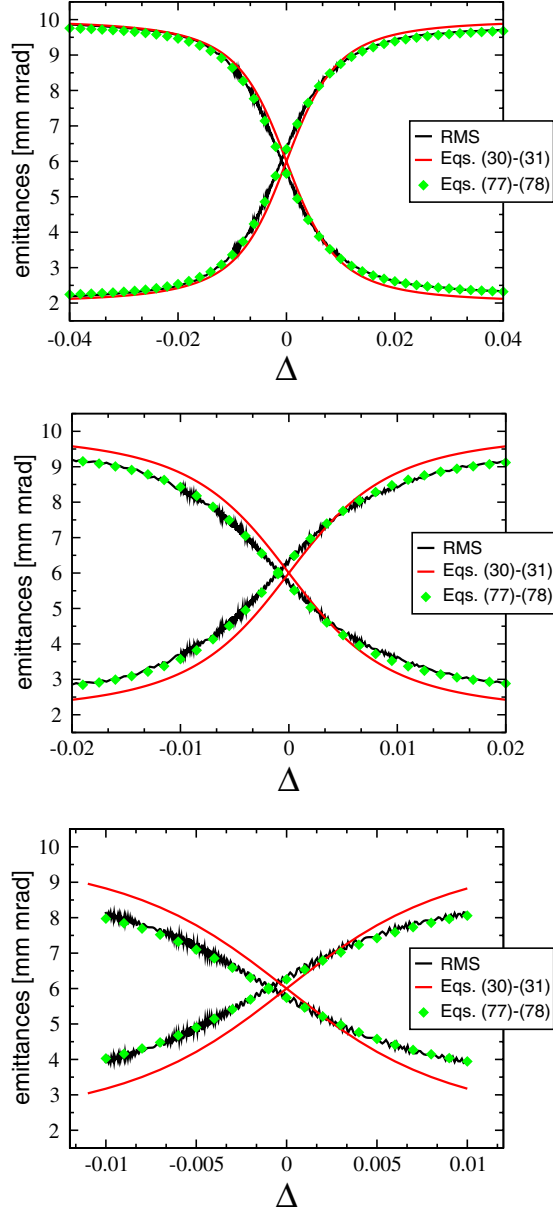
FIG. 7. (Color) Dynamical crossing from multiparticle simulations: the RMS emittances are plotted together with Eqs. (77) and (78) and Eqs. (30) and (31) for several starting points. The coupling strength is $|C| = 0.01$.

for Eqs. (30) and (31). As shown in Fig. 7 the agreement between the RMS emittances computed from multiparticle simulations and new formulas remains excellent for any starting point.

Equations (30) and (31) are derived assuming a starting point far enough from the resonance stop band, such that $f_0 \approx 0$, $c_h \approx \epsilon_{x0}$, and $c_v \approx \epsilon_{y0}$. We also rewrite T_f as

$$\sin^2(2f) = \frac{1 - \cos(4f)}{2} = \frac{1 - \sqrt{1 - \sin^2(4f)}}{2}, \qquad (82)$$

$$\cos^2(2f) = \frac{1 + \cos(4f)}{2} = \frac{1 + \sqrt{1 - \sin^2(4f)}}{2}. \qquad (83)$$

Substituting $\sin^2(4f) \approx 16\bar{f}$ as done in Eq. (61), after some algebra we obtain

$$\sin^2(2f) \approx \frac{1}{2}\frac{|C_0|^2}{\Delta^2 + |C|^2 + |\Delta|\sqrt{\Delta^2 + |C|^2}}, \qquad (84)$$

$$\cos^2(2f) \approx \frac{1}{2}\frac{|C_0|^2}{\Delta^2 + |C|^2 - |\Delta|\sqrt{\Delta^2 + |C|^2}}, \qquad (85)$$

with C_0 defined in Eq. (58). Under these assumptions Eqs. (77) and (78) read

$$\epsilon_x = \epsilon_{x0} + \frac{|C_0|^2}{\Delta^2 + |C|^2 \pm \Delta\sqrt{\Delta^2 + |C|^2}}\frac{\epsilon_{y0} - \epsilon_{x0}}{2}, \qquad (86)$$

$$\epsilon_y = \epsilon_{y0} - \frac{|C_0|^2}{\Delta^2 + |C|^2 \pm \Delta\sqrt{\Delta^2 + |C|^2}}\frac{\epsilon_{y0} - \epsilon_{x0}}{2}. \qquad (87)$$

The sign in the denominator depends on the crossing direction. Equations (30) and (31) are eventually obtained expanding $|C_0|^2 \approx |C|^2$ as done for the static case.

V. COMPUTING AND MEASURING f_{1001}

The approximate expression of f_{1001} given in Eq. (40) might not be accurate enough close to the resonance. This relation is indeed derived from a first-order normal form, and higher order contributions need to be taken into account. Nevertheless, Eqs. (38) and (39) provide a direct way to compute $f_{1001} = fe^{iq}$: the spectrum of turn-by-turn oscillations of the beam centroid contains two peaks in each plane, namely

$$H(1, 0) = \cos(2f)\sqrt{2I_x}e^{i\psi_{x0}}$$

$$H(0, 1) = -ie^{iq}\sin(2f)\sqrt{2I_y}e^{i\psi_{y0}}$$

$$V(0, 1) = \cos(2f)\sqrt{2I_y}e^{i\psi_{y0}}$$
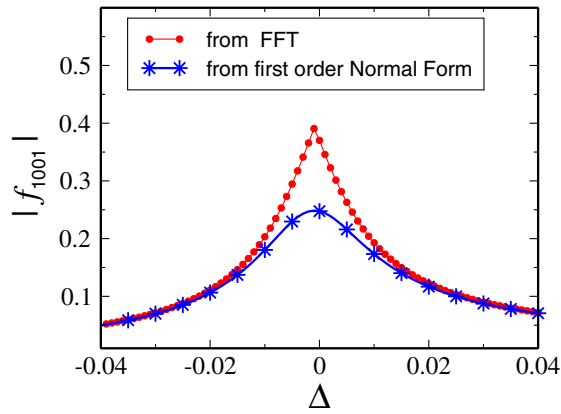
$$V(1, 0) = -ie^{-iq}\sin(2f)\sqrt{2I_x}e^{i\psi_{x0}}.$$

FIG. 8. (Color) $|\bar{f}_{1001}|$ from Eq. (40) (blue line) compared with $|f_{1001}|$ from Eq. (88) against Δ. Note how on the resonance, $\Delta = 0$, $|\bar{f}_{1001}| = 1/4$ whereas $|f_{1001}| = \pi/8$. The coupling strength is $|C| = 0.02$

It is easy to prove that

$$\tan 2f = \sqrt{\frac{|H(0,1)||V(1,0)|}{|H(1,0)||V(0,1)|}}, \qquad (88)$$

$$q = \phi_{H(0,1)} - \phi_{V(0,1)} + \frac{\pi}{2} = \phi_{H(1,0)} - \phi_{V(1,0)} - \frac{\pi}{2}, \qquad (89)$$

where $\phi_{V(m,n)}$ and $\phi_{H(m,n)}$ are the phases of the spectral peaks $V(m,n)$ and $H(m,n)$, respectively. f_{1001} can be therefore inferred from the harmonic analysis of $h_{x,y}(N)$ inverting the above relations. It can be shown [10] that Eq. (88) is free from BPM calibration error, as well as Eq. (89) is independent of phase shift. In Fig. 8 the exact $|f_{1001}|$ as computed from the above relations for $|C| = 0.02$ is plotted against Δ and compared with the first-order expression $|\bar{f}_{1001}|$ given in Eq. (40), which is directly computed from the lattice model. Note that for $\Delta \geq |C|$ the two formulas are equivalent.

An alternative way to measure both Δ_e and $|f_{1001}|$ is given by using fast turn-by-turn emittance monitors, after fitting the turn-by-turn oscillations of the RMS emittances with Eqs. (54) and (55). If the emittance measurement averages over many turns, Δ_e is no longer observable. Nevertheless $|f_{1001}|$ is still measurable from Eqs. (56) and (57), see [12,16].

VI. MEASUREMENT OF EMITTANCE EXCHANGE IN THE CERN PS

Emittance exchange has been already observed experimentally at the CERN PS [7], where the emittances have been measured with wire scanners during a machine cycle set to cross the difference resonance. Measurements have been performed on the injection flat-bottom at 2.14 GeV/c, where the machine nonlinearities are well under control [18]. The number of protons per

bunch was $N_b \approx 7 \times 10^{11}$, yielding to the following incoherent space-charge tune shifts, $\Delta Q_{\text{inc},x0} \approx -0.05$ and $\Delta Q_{\text{inc},y0} \approx -0.09$.

Trying to replot the analytical predictions for the PS experiment, an error in the postprocessing was discovered. An even better agreement between theory and measurements is now obtained.

In the upper plot of Fig. 9, the tune ramp set in the control room is shown: both tunes have been slowly varied for 100 ms between 6.1 and 6.3 in order to cross the resonance at 6.2. In the bottom plot, the measured eigentunes are shown. Betatron coupling is controlled by powering a string of skew quadrupoles and is independently measured with the closest-tune approach ($|C| = 0.055$ in the plot). The physical emittances at 2σ measured before the crossing are $\epsilon_{x0} = 9.5$ mm rad and $\epsilon_{y0} = 3.6$ mm rad, respectively. In Fig. 10 the emittance curves for the case corresponding to the setting of Fig. 9 are shown: the overall agreement between the experimental data and Eqs. (30) and (31) is remarkable. Each point in the plot represents an average over three machine cycles and the error bars are introduced to include the wire scanner accuracy of about 10%, which is the same contribution to the horizontal emittance induced by dispersion.

The robustness of Eqs. (30) and (31) has been tested for several coupling strengths. In Fig. 11 the two extreme cases are shown. In the upper plot a slow exchange occurs as a consequence of a large coupling, $|C| = 0.120$. In the bottom plot instead, the emittances exchange rapidly
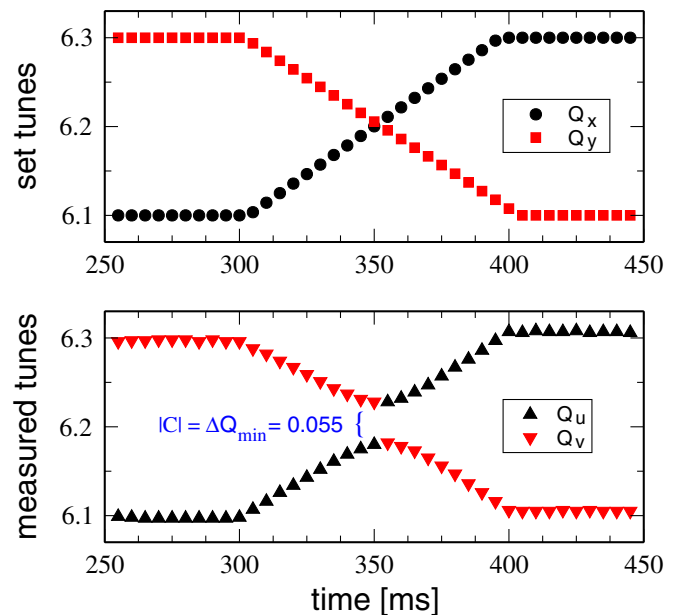

FIG. 9. (Color) Time dependence of the tunes $Q_{x,y}$ as set in the control room to cross the resonance (upper plot). Measured eigentunes $Q_{u,v}$ for the case with the skew quadrupole current of -0.5 A (bottom plot): the resulting coupling strength $|C| = 0.055$ is inferred from the closest-tune approach.
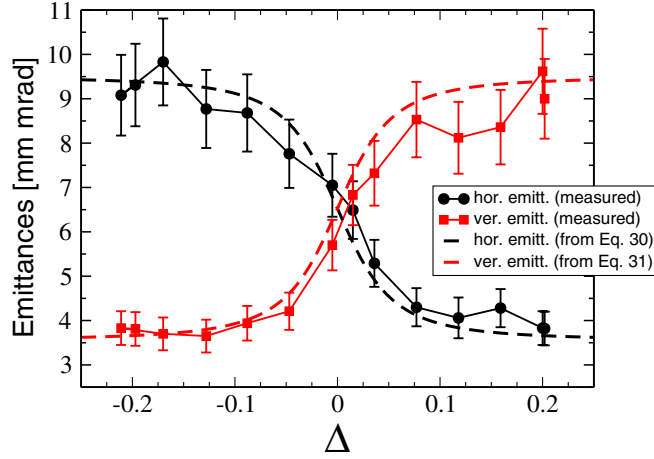
A. FRANCHI, E. MÉTRAL, AND R. TOMÁS

Phys. Rev. ST Accel. Beams **10,** 064003 (2007)

FIG. 10. (Color) Transverse physical emittances at 2σ measured in the PS while crossing the resonance with a coupling strength $|C| = 0.055$. The dashed lines correspond to the curves predicted by Eqs. (30) and (31).
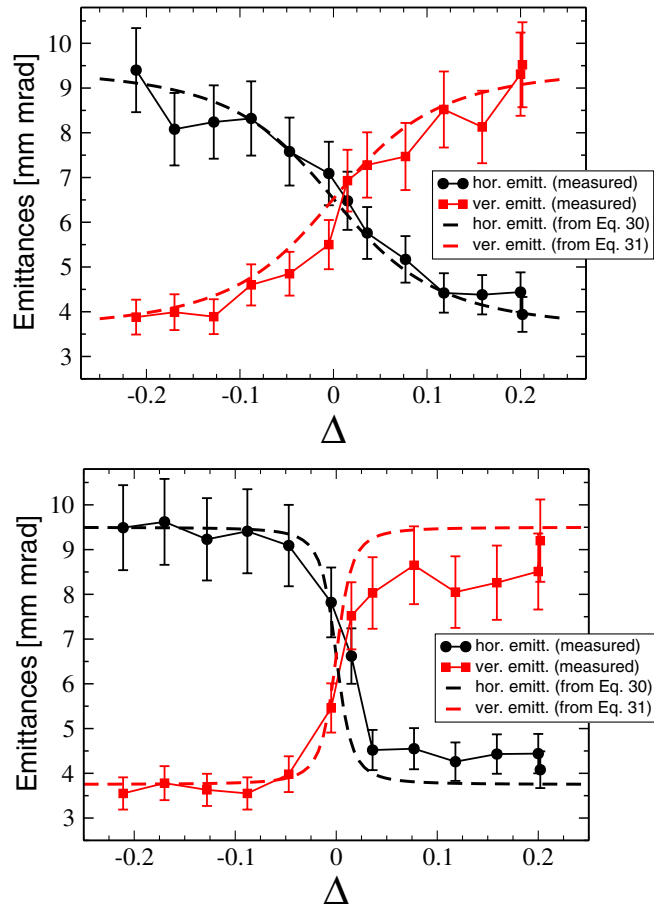

FIG. 11. (Color) Emittance-exchange curves measured in the PS for two extreme cases with large coupling, $|C| = 0.120$ (upper plot), and small coupling, $|C| = 0.016$ (bottom plot). The dashed lines correspond to the curves predicted by Eqs. (30) and (31). The curves denote the physical emittances at 2σ.

(~ 10 ms) because of the small coupling, $|C| = 0.016$ (the crossing speed was the same during all the measurements, see discussion in Sec. III). This might explain the poorer agreement with the theoretical prediction on the right side of the resonance, as the fast exchange might drive a temporary mismatch while ending the crossing. Another source of discrepancies (not included in our model) might be space charge, through the Montague resonance. In [9] it was observed that in a decoupled machine space charge leads to a transverse emittance exchange, which may be not complete if the synchrotron period (1.2 ms in the measurement) is smaller or comparable with the crossing time. The partial exchange, together with the large tune shift ($\Delta Q_{inc,y0} \approx -0.09$) and the small coupling ($|C| = 0.016$), indicates that the curves in the bottom plot of Fig. 11 might be the result of a combined effect of linear betatron coupling and space charge.

VII. CONCLUSION

New formulas have been derived in the smooth approximation, as well as in a strong-focusing lattice with localized skew quadrupole fields, which describe the effect of betatron coupling on the transverse emittances. By crossing the difference resonance $Q_x - Q_y - l = 0$ the two emittances exchange completely. The agreement between theory and experimental results is remarkable. The use of both the Lie algebra and the resonance driving terms formalism explains some counterintuitive effects observable in multiparticle simulations, such as the emittance variation around the ring due to strong localized sources of coupling and the asymmetry in the emittance sharing curve.

ACKNOWLEDGMENTS

APPENDIX: LIE SERIES WITH BETATRON COUPLING

In [10,11] the turn-by-turn normalized particle positions and momenta in a coupled lattice are described as follows:

$$h_x = \hat{x} - i\hat{p}_x$$
$$= \sqrt{2I_x}e^{i\psi_x} - 2if_{1001}\sqrt{2I_y}e^{i\psi_y} - 2if_{1010}\sqrt{2I_y}e^{-i\psi_y},$$

$$(A1)$$

$$h_y = \hat{y} - i\hat{p}_y$$
$$= \sqrt{2I_y}e^{i\psi_y} - 2if_{1001}^*\sqrt{2I_x}e^{i\psi_x} - 2if_{1010}\sqrt{2I_x}e^{-i\psi_x},$$
$$\text{(A2)}$$

where $I_{x,y}$ are the horizontal and the vertical invariants, $\psi_{x,y}$ are the phases of the oscillations which can be expressed as function of the fractional part of the eigentunes $Q_{u,v}$, the turn number N, and the initial phases $\phi_{x0,y0}$ as $\psi_{x,y} = 2\pi Q_{u,v}N + \phi_{x0,y0}$.

Equations (A1) and (A2) apply to linear lattice in the presence linear betatron coupling, where the RDTs f_{1010} and f_{1001} drive the sum resonance ($Q_x + Q_y = 0$) and the difference resonance ($Q_x - Q_y = 0$), respectively. However they are truncated to the first order. This truncation is legitimate as long as betatron coupling is weak and the distance from the resonance is larger than the stop band, $\Delta \ge |C|$.

In this Appendix we derive a closed expansion that removes these assumptions. The Lie expansion of h_x reads [17]

$$h_x = e^{:F:}\zeta_x^- = \sum_{n=0}^{\infty} \frac{D_F^n \zeta_x^-}{n!}$$

$$= \zeta_x^- + [F, \zeta_x^-] + \frac{1}{2!}[F, [F, \zeta_x^-]] + \cdots, \quad \text{(A3)}$$

where $\zeta^- = \sqrt{2I}e^{i\psi}$ are the normal form coordinates; $D_F\zeta_x^- = [F, \zeta^-]$ denotes the Poisson bracket; F is the generating function for the normal form transformation. In case of betatron coupling this function reads

$$F = f_{1001}\zeta_x^+ \zeta_y^- + f_{1001}^*\zeta_x^- \zeta_y^+ + f_{1010}\zeta_x^+ \zeta_y^+$$
$$+ f_{1010}^*\zeta_x^- \zeta_y^-. \quad \text{(A4)}$$

The reason why only these four terms are considered here is the following. To the first order, a generic potential $x^G y^D$ drives all the resonance terms f_{jklm} such that $j + k = G$ and $l + m = D$ [17]. In the case of a skew quadrupolar potential $\propto xy$, this corresponds to the resonance terms of Eq. (A4). It can be shown that second-order terms of this potential induce a normal quadrupole component. The latter is the one responsible for the detuning $Q_{x,y} \to Q_{u,v}$ and for a change of the linear optics that, however, does not affect the following derivation, as we start already from the Courant-Snyder coordinates.

The Poisson brackets of Eq. (A3) can be made explicit with a recursive relation (note that $[\zeta_x^+, \zeta_x^-] = [\zeta_y^+, \zeta_y^-] = -2i$, all other combinations being zero):

$$D_F^1 \zeta_x^- = [F, \zeta_x^-] = [f_{1001}\zeta_x^+ \zeta_y^- + f_{1010}\zeta_x^+ \zeta_y^+, \zeta_x^-] = -2if_{1001}\zeta_y^- - 2if_{1010}\zeta_y^+,$$

$$D_F^2 \zeta_x^- = [F, D_F^1 \zeta_x^-] = [-|2f_{1001}|^2 + |2f_{1010}|^2]\zeta_x^-,$$

$$D_F^3 \zeta_x^- = [F, D_F^2 \zeta_x^-] = [-|2f_{1001}|^2 + |2f_{1010}|^2](-2if_{1001}\zeta_y^- - 2if_{1010}\zeta_y^+),$$

$$D_F^4 \zeta_x^- = [F, D_F^3 \zeta_x^-] = [-|2f_{1001}|^2 + |2f_{1010}|^2]^2\zeta_x^-,$$

$$\vdots$$

$$D_F^{2n} \zeta_x^- = (2\mathcal{P})^{2n}\zeta_x^-, \quad \text{(A5)}$$

$$D_F^{2n+1} \zeta_x^- = -i(2\mathcal{P})^{2n+1}\left(\frac{f_{1001}}{\mathcal{P}}\zeta_y^- + \frac{f_{1010}}{\mathcal{P}}\zeta_y^+\right), \quad \text{(A6)}$$

where

$$2\mathcal{P} = \sqrt{-|2f_{1001}|^2 + |2f_{1010}|^2}. \quad \text{(A7)}$$

The Lie series in Eq. (A3) therefore reads

$$h_x = \left(\sum_{n=0}^{\infty}\frac{(2\mathcal{P})^{2n}}{(2n)!}\right)\zeta_x^- - i\left(\sum_{n=0}^{\infty}\frac{(2\mathcal{P})^{2n+1}}{(2n+1)!}\right)$$
$$\times \left[\frac{f_{1001}}{\mathcal{P}}\zeta_y^- + \frac{f_{1010}}{\mathcal{P}}\zeta_y^+\right].$$

The summations in the above rhs are the Taylor expansions of $\cosh(2\mathcal{P})$ and $\sinh(2\mathcal{P})$, respectively, providing

$$h_x = \cosh(2\mathcal{P})\zeta_x^- - i\sinh(2\mathcal{P})\left[\frac{f_{1001}}{\mathcal{P}}\zeta_y^- + \frac{f_{1010}}{\mathcal{P}}\zeta_y^+\right],$$
$$\text{(A8)}$$

$$h_y = \cosh(2\mathcal{P})\zeta_y^- - i\sinh(2\mathcal{P})\left[\frac{f_{1001}^*}{\mathcal{P}}\zeta_x^- + \frac{f_{1010}}{\mathcal{P}}\zeta_x^+\right],$$
$$\text{(A9)}$$

where the expression for h_y has been obtained with a similar derivation. Notice that expanding the hyperbolic functions up to the first order, Eqs. (A1)–(A3) are retrieved.

In the context of this paper two limit cases are of interest. First, consider the case with a tune working point close to the sum resonance (1,1) and betatron coupling such that $|f_{1001}| \ll |f_{1010}|$. In this case $\mathcal{P} \to |f_{1010}|$ and the Courant-Snyder coordinates read

A. FRANCHI, E. MÉTRAL, AND R. TOMÁS

Phys. Rev. ST Accel. Beams **10,** 064003 (2007)

$$h_x = \cosh(2|f_{1010}|)\zeta_x^- - ie^{id}\sinh(2|f_{1010}|)\zeta_y^+, \quad \text{(A10)}$$

$$h_y = \cosh(2|f_{1010}|)\zeta_y^- - ie^{id}\sinh(2|f_{1010}|)\zeta_x^+, \quad \text{(A11)}$$

where d is the phase of f_{1010}. It is easy to prove that in this case the difference between the two single-particle emittances is invariant,

$$E_x - E_y = |h_x|^2 - |h_y|^2 = 2I_x - 2I_y, \quad \text{(A12)}$$

while the hyperbolic functions drive an emittance blowup when approaching the resonance. A completely different behavior occurs in the second limit case, when, close to the difference resonance $(1, -1)$, $|f_{1010}| \ll |f_{1001}|$. In this case $\mathcal{P} \to i|f_{1001}|$ and the Courant-Snyder coordinates read

$$h_x = \cos(2|f_{1001}|)\zeta_x^- - ie^{iq}\sin(2|f_{1001}|)\zeta_y^-, \quad \text{(A13)}$$

$$h_y = \cos(2|f_{1001}|)\zeta_y^- - ie^{-iq}\sin(2|f_{1001}|)\zeta_x^-, \quad \text{(A14)}$$

where q is the phase of f_{1001}. It is easy to prove that in this case the no emittance blowup is induced and that the sum of the two single-particle emittances is invariant,

$$E_x + E_y = |h_x|^2 + |h_y|^2 = 2I_x + 2I_y. \quad \text{(A15)}$$

Making explicit ζ in Eqs. (A13) and (A14), the following turn-by-turn relations are obtained

$$h_x(N) = \cos(2f)\sqrt{2I_x}e^{i(2\pi NQ_u + \psi_{x0})}$$
$$- ie^{iq}\sin(2f)\sqrt{2I_y}e^{i(2\pi NQ_v + \psi_{y0})}, \quad \text{(A16)}$$

$$h_y(N) = \cos(2f)\sqrt{2I_y}e^{i(2\pi NQ_v + \psi_{y0})}$$
$$- ie^{-iq}\sin(2f)\sqrt{2I_x}e^{i(2\pi NQ_u + \psi_{x0})}, \quad \text{(A17)}$$

where $f = |f_{1001}|$, N is the turn number, $Q_{u,v}$ are the eigentunes, and $\psi_{x0,y0}$ are the initial particle phases in normal form.

[1] K. Schindl and P. van der Stok, CERN/PS/BR 76-19, 1976.
[2] G. Guignard, CERN ISR-BOM/77-43, 1977.
[3] D. Edwards and L. C. Teng, IEEE Trans. Nucl. Sci. **20**, 885 (1973).
[4] D. Chernin, Part. Accel. **24**, 29 (1988).
[5] L. C. Teng, Proceedings of PAC 2003, Portland, p. 2895.
[6] A. Wolsky, Phys. Rev. ST Accel. Beams **9**, 024001 (2006).
[7] C. Carli, G. Cyvoct, M. Giovannozzi, E. Métral, and R. Steerenberg, Proceedings of EPAC 2002, Paris, p. 1157.
[8] G. Franchetti, I. Hofmann, M. Giovannozzi, M. Martini, E. Metral, J. Qiang, and R. D. Ryne, *Simulation Aspects of the Code Benchmarking Based on the CERN-PS "Montague-resonance" Experiment*, AIP Conf. Proc. No. 773 (AIP, New York, 2005), pp. 169–171.
[9] E. Métral, G. Franchetti, I. Hofmann, M. Giovannozzi, M. Martini, R. Steerenberg, J. Qiang, and R. D. Ryne, Proceedings of EPAC 2004, Lucerne, 2004, p. 1894; *Space-Charge Experiments at the CERN Proton Synchrotron*, AIP Conf. Proc. No. 773 (AIP, New York, 2005), pp. 122–126.
[10] R. Tomás García, Ph.D. thesis, University of Valencia, Spain, 2003, CERN-THESIS-2003-010.
[11] R. Calaga, R. Tomás García, and A. Franchi, Phys. Rev. ST Accel. Beams **8**, 034001 (2005).
[12] M. Minty and F. Zimmermann, *Measurement and Control of Charged Particle Beams* (Springer, Berlin, 2003), ISBN 3-540-44197-5.
[13] G. Franchetti, I. Hofmann, and G. Turchetti, AIP Conf. Proc. **448**, 233 (1998).
[14] E. Métral, CERN/PS 2001-066(AE), 2001.
[15] A. Bazzani, E. Todesco, G. Turchetti, and G. Servizi, CERN 94-02, 1994.
[16] A. Franchi, Ph.D. thesis, J. W. Goethe University, Frankfurt am Main, Germany, GSI DISS 2006-07, 2006.
[17] R. Bartolini and F. Schmidt, Part. Accel. **59**, 93 (1998).
[18] R. Cappi, M. Giovannozzi, M. Martini, E. Metral, G. Metral, R. Steerenberg, and A. S. Muller, Proceedings of PAC 2003, Portland, p. 2913.